CSIRO PUBLISHING
www.publish.csiro.au/journals/eg
Exploration Geophysics, 2007, **38**, 19–28

Multi-station joint inversion of receiver function and surface-wave phase velocity data for exploration of deep sedimentary layers

Takeshi Kurose[1,2,3] Hiroaki Yamanaka[1,3]

[1]Interdisciplinary Graduate School of Science and Engineering, Tokyo Institute of Technology, 4259, Nagatsuta-cho, Midori-ku, Yokohama, Kanagawa 226-8502, Japan.
[2]Currently: ITOCHU Techno-Solutions Corporation, 2-7-5, Minamisuna, Koto-ku, Tokyo 136-8581, Japan.
[3]Corresponding authors. Emails: yamanaka@depe.titech.ac.jp; takeshi.kurose@ctc-g.co.jp

Abstract. In this study, we propose a joint inversion method, using genetic algorithms, to estimate an S-wave velocity structure for deep sedimentary layers from receiver functions and surface-wave phase velocity observed at several sites. The method takes layer continuity over a target area into consideration by assuming that each layer has uniform physical properties, especially an S-wave velocity, at all the sites in a target area in order to invert datasets acquired at different sites simultaneously. Numerical experiments with synthetic data indicate that the proposed method is effective in reducing uncertainty in deep structure parameters when modelling only surface-wave dispersion data over a limited period range. We then apply the method to receiver functions derived from earthquake records at one site and two datasets of Rayleigh-wave phase velocity obtained from microtremor array surveys performed in central Tokyo, Japan. The estimated subsurface structure is in good agreement with the results of previous seismic refraction surveys and deep borehole data. We also conclude that the proposed method can provide a more accurate and reliable model than individual inversions of either receiver function data only or surface-wave dispersion data only.

Key words: genetic algorithms, microtremor array survey, multi-station joint inversion, phase velocity, receiver function, surface wave, S-wave velocity.

Introduction

Microtremor array surveying has been developed as a method to estimate the S-wave velocities of deep sedimentary layers from inversion of Rayleigh wave phase velocity (Horike, 1985; Okada, 2003). Recently, three-dimensional models of deep subsurface structure have been constructed from S-wave velocity profiles obtained from microtremor array surveys performed at several sites in large-scale sedimentary basins in Japan (e.g. Kagawa et al., 1998; Yamanaka and Yamada, 2002). However, the range of periods in observed microtremor data is generally limited because of the inherently small amplitudes of long-period microtremor and the limited array aperture. This limitation gives rise to uncertainty in deep structure determined by phase velocity inversion. Yamanaka et al. (1995) found out that Rayleigh-wave phase-velocity inversion of data up to a period of 5 s only, acquired by a microtremor array survey in central Tokyo, Japan, resulted in low resolution of deep structure. They, however, inverted the Rayleigh-wave dispersion data simultaneously with Love-wave phase velocities up to a period of 10 s, obtained from earthquake records, and found that the resolution of deep structure was improved. In order to overcome the unavailability of enough long-period phase velocity data, Feng et al. (2003) proposed a multi-station inversion method in order to analyse simultaneously several datasets of Rayleigh-wave phase velocity, obtained from microtremor array surveys conducted at several different sites. They pointed out the difficulty of correlation of subsurface layers between adjacent sites after a conventional inversion of phase velocity dispersion at each site. They assumed that each layer was continuous over a target area, which is represented by relationship equations, and that the noise contained in the datasets observed at each site was uncorrelated from site to site. Using both numerical experiments and analysis of actual field data, they indicated that their method can reduce the effect of noise and improve the correlation of each layer across the target area. As for the uncertainty of inversion results in microtremor array technique, Cho et al. (1999) also point out that there is a trade-off between shallower and deeper parameters, which may cause non-uniqueness in resulting models.

The receiver-function method was originally developed to explore the S-wave velocity structure of the crust and mantle (Langston, 1979). Receiver function inversions (Owens et al., 1984) have been used by many researchers for crust and mantle studies (e.g. Darbyshire et al., 2000; Last et al., 1997; Priestley et al., 1988). Recently, the receiver function has received attention from earthquake engineers as a method of detecting P-S converted waves generated at the sediment/basement boundary (Kobayashi et al., 1998). They pointed out that P-S converted waves detected from receiver functions well constrain the deeper structure of sedimentary layers over the basement. However, it is well known that receiver function inversion results may suffer from non-uniqueness because of a trade-off between S-wave velocities and thicknesses (Ammon et al., 1990). In order to settle the trade-off problem, some crust and mantle studies have conducted a joint inversion of receiver functions and surface-wave dispersion observations (e.g. Julia et al., 2000; Chang et al., 2004). We have also proposed a joint inversion method for receiver functions and surface-wave phase velocity dispersion, using a genetic algorithm (GA), in order to apply receiver function inversion to exploring deeper sedimentary layers, and to resolve the trade-off problems that arise when modelling only one kind of observed data (Kurose and Yamanaka, 2006).

10.1071/EG07007 0812-3985/07/010019

In this study, we propose a multi-station joint inversion method that can model simultaneously receiver function and surface-wave phase velocity datasets acquired at several different sites, to determine an S-wave velocity structure for deep sedimentary layers, taking the continuity of layers in the target area into consideration. In practice, surface-wave dispersion data are used mainly to constrain the shallower structure, while receiver function data are utilised chiefly to determine the deeper structure. In essence, our method combines the concepts and methods of the multi-station inversion method for microtremor array surveys developed by Feng et al. (2003) with the joint inversion method for receiver functions and surface-wave phase velocities devised by Kurose and Yamanaka (2006). The latter is referred to as 'our previous paper' in the following.

Multi-station joint inversion method

Here we present our multi-station joint inversion method for receiver function and surface-wave phase velocity data, observed at several different sites on a common sedimentary basin. We use a genetic algorithm to simultaneously determine one-dimensional S-wave velocity profiles at each site that can account for the dataset acquired at that site.

Figure 1 illustrates the fundamental concept of our method. In order to simultaneously invert datasets obtained at several different sites, we consider each layer in the target area to be continuous. To take layer continuity into consideration, Feng et al. (2003) proposed a method using relationship equations to constrain the unknown parameters at adjacent sites, such as allowing the S-wave velocity of the same layer in the target area to change only in the range of ±20%. In this study, we make the simpler assumption that the S-wave velocity in each layer is uniform across the target area. Although this assumption may be a very strong constraint condition in the inversion, it does provide useful models with which to construct a 3D model with homogeneous layers such as are often used in earthquake motion simulation in strong motion seismology. The assumption seems to be effective, when applied to an area with a large accumulation of receiver function analyses and/or microtremor array surveys, in integrating the profiles at each site from individual inversions into a more precise and less obscure subsurface structural model over the area. On the other hand, if the assumption is inappropriate, the inversion may lead to a distorted subsurface structural model. In addition, the strength of the constraint condition (uniformity of S-wave velocity in each layer) may depend on the spatial distribution of observation sites and on the kinds of observed data. Hence, our multi-station joint inversion method must be investigated from many viewpoints. In this study, we focus on how it works when applied to an area with surface-wave dispersion data observed only in a limited period range.

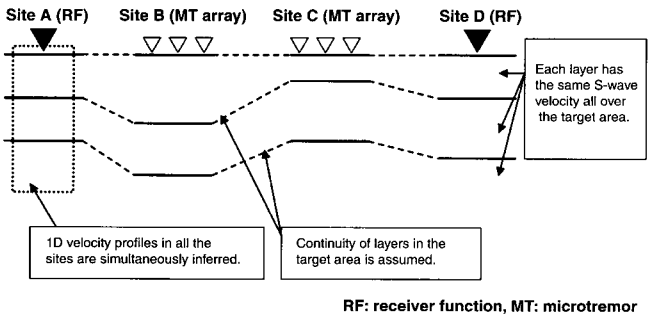

Fig. 1. Schematic diagram of the method of multi-station joint inversion of receiver function and surface-wave phase velocity data, taking layer continuity into consideration.

We parameterise S-wave velocities and thicknesses in our inversion, as shown in the following, which results in a model in which the S-wave velocities are common at all the sites while thicknesses are different site by site. For example, in the case of three-layer model in Figure 1, the number of parameters to be determined by our method is 11, comprising three S-wave velocities (including the velocity in the half-space, corresponding with the basement) and two thicknesses at the four sites.

The objective function (misfit) to be minimised in the inversion is defined as follows. Provided that there are N_{RF} sites where receiver functions are obtained, and N_{ph} sites for Rayleigh-wave phase velocity, the misfit $\phi_{RF}^{(i)}$ for the receiver function at the i-th site, and the misfit $\phi_{ph}^{(j)}$ for the phase velocity at the j-th site, are defined in equation (1).

$$\phi_{RF}^{(i)} = \frac{1}{L_{RF}^{(i)}} \sum_{k} \left(\frac{R_{obs}^{(i)}(t_k) - R_{cal}^{(i)}(t_k)}{\sigma_{RF}^{(i)}(t_k)} \right)^2$$
$$\phi_{ph}^{(j)} = \frac{1}{L_{ph}^{(j)}} \sum_{m} \left(\frac{C_{obs}^{(j)}(T_m) - C_{cal}^{(j)}(T_m)}{\sigma_{ph}^{(j)}(T_m)} \right)^2 \quad (1)$$

Here, $L_{RF}^{(i)}$ and $L_{ph}^{(j)}$ are the number of data, and $\sigma_{RF}^{(i)}(t_k)$ and $\sigma_{ph}^{(j)}(T_m)$ are the standard deviations of the receiver function observed at the i-th site $R_{obs}^{(i)}(t_k)$ at time t_k, and of the phase velocity observed at the j-th site $C_{obs}^{(j)}(T_m)$ at period T_m, respectively. The misfit ϕ to be minimised in the inversion is defined by equation (2).

$$\phi = \frac{\sum_{j=1}^{N_{ph}} \phi_{ph}^{(j)} + \sum_{i=1}^{N_{RF}} \phi_{RF}^{(i)}}{N_{ph} + N_{RF}} \quad (2)$$

This shows that the misfit to be minimised in the inversion is the average of misfit derived at all the sites, which reflects the indication that receiver function and surface-wave phase velocity equivalently constrain the S-wave velocity profile, as suggested in our previous paper.

In the inversion, S-wave velocities and thicknesses are inferred so that the misfit defined by equation (2) will be minimised. Synthetic receiver functions and surface-wave phase velocity values can be calculated using P- and S-wave velocities, thicknesses, and densities of each layer in a flat-layered model. However, S-wave velocities and thicknesses are the most influential (e.g. Horike, 1985; Owens et al., 1984). Therefore, we allow S-wave velocities and thicknesses to vary in the inversion, as mentioned earlier, and calculate P-wave velocities from S-wave velocities using an empirical relationship derived from velocity data for deep sedimentary layers in Japan by Kitsunezaki et al. (1990). Densities are fixed, constant values in each layer. The theoretical receiver function and the theoretical phase velocity, $R_{cal}^{(i)}(t_k)$ and $C_{cal}^{(j)}(T_m)$ in equation (1), are calculated by the methods of Haskell (1962) and Haskell (1953), respectively.

The GA we have implemented here is similar to that of Yamanaka and Ishida (1996), who adopted an eight-bit binary coding of each parameter, elite selection, roulette-rule selection, and dynamic mutation. Dynamic mutation is an operation that changes the mutation rate at each generation depending on how the parameters of all the individuals have converged (Yamanaka and Ishida, 1996). The GA parameters we employed were: crossover rate 0.9, mutation rate 0.01, and population size 100 in the numerical experiments. We used a population size of 200

in the analysis of actual observed data. Other conditions of the genetic inversion and the method used to evaluate the inversion result are the same as in our previous paper. Further details of the GA implemented here can be found in Yamanaka and Ishida (1996).

Numerical experiment

We performed a numerical experiment with our method to investigate its applicability in the case where there are not enough long-period phase velocity data available, which may often happen in real microtremor array surveys. The subsurface structural model used in the numerical experiment is shown in Table 1. This is a model of deep sedimentary layers down to a basement with an S-wave velocity of ~3 km s^{-1}, typical of conditions in and around Tokyo, Japan (e.g. Yamanaka and Yamada, 2002). The model assumes that two adjacent sites have different thicknesses but common S-wave velocities so that we can validate the applicability of our multi-station joint inversion method. Theoretical receiver function data were calculated for the site A model, and fundamental-mode Rayleigh-wave phase velocities for the structure at site B. In order to simulate the situation where phase velocity data are not perfectly observed in an actual survey, we used only the phase velocity at periods shorter than 4.5 s. After they were contaminated with two sets of random noise, as shown in Figure 2, these synthetic datasets were used in the numerical test. The noise added to the receiver function data lies in the range of ±0.2, while we added 10% noise to the phase velocity at each data point. The incident angle for the derivation of receiver function data was set to be 40°. This value was calculated using a P-wave velocity structure of the crust and mantle modified from the model used in epicentre determination by the Earthquake Research Institute of the University of Tokyo, shown in our previous paper. We assumed an event with an epicentral distance of ~100 km and a focal depth of ~20 km in the calculation of the incident angle. The data were also band-pass filtered in a period range of 0.5 to 5.0 s. We also supposed frequency-independent Q-values, Q_p and Q_s, defined as 1/15 of P- and S-wave velocities, respectively. The standard deviation of the receiver function was set to be 0.2 uniformly, while that of the phase velocity was set to be 10% of the contaminated synthetics. Search limits for the GA inversion for each parameter were set as displayed in Table 1, and the two datasets were also individually inverted for comparison. A population size of 30 was used in the individual inversion, which is about a third of the size used in the multi-station joint inversion, but the other GA parameters were as given above. We also fixed the S-wave velocity of the basement to be constant, as existing receiver function and surface-wave dispersion studies (e.g. Yamanaka and Yamada, 2002; Chang et al., 2004) suggest that the S-wave velocity of the half-space cannot be resolved well enough in the final model.

S-wave velocity structures obtained from the individual inversions are shown in Figure 3. These show that the individual inversion of receiver function data fairly well reproduced the true model, with a small deviation in each parameter. However, there is a comparatively large discrepancy between the true model and the one obtained by individual inversion of the phase velocity data, especially in the deep part of the model. On the other hand, the multi-station joint inversion did well in reconstructing the true model both at Site A and at Site B, as presented in Figure 4. In particular, the thickness of the third layer at Site B is much better determined than by the individual inversion of the phase-velocity data. It is considered that, in multi-station joint inversion, the assumption of layer continuity plays a strong constraining role, which is similar to the case of 'single-station' joint inversion in our previous paper. Figure 5 shows the comparison between the data devised for the numerical test and the synthetic data derived from the multi-station joint inversion result, which demonstrates that the inversion result does account well for the test data.

Next, as in our previous paper, we evaluate the uniqueness of the inversion results by using the concept of acceptable solutions. This method selects those models with misfits lower than a misfit threshold as acceptable solutions, from all the models explored in the GA inversion, and approximately evaluates the uniqueness of the inversion result from the parameter distributions of the selected models (Lomax and Snieder, 1994). Refer to our previous paper for detailed information on this method.

The distributions of parameters are displayed in Figure 6, for the acceptable models found by individual inversions of receiver function and phase velocity data. The misfit threshold for acceptable solutions was set to be equal to the minimum misfit plus 0.01, determined by trial-and-error. In Figure 6a, almost all the models plot on straight lines, indicating a constant ratio between S-wave velocities and thicknesses. This linear relationship is attributed to the trade-off between S-wave velocities and thicknesses in receiver function inversion (Ammon et al., 1990). In Figure 6b, the parameters for the acceptable solutions for the second and third layers are distributed in comparatively large clusters, suggesting lesser resolution of deep structure than of the first layer.

Figure 7 presents the parameter distributions for acceptable models acquired by multi-station joint inversion. At Site A, the parameters for the first and the second layers are distributed near single points, showing that the effect of the trade-off was considerably suppressed in these layers, as compared with the inversion of the receiver function only. At Site B, the parameters of the acceptable solutions for every layer in the multi-station joint inversion are distributed in a smaller area than those from the inversion of phase velocity alone, particularly for the third layer. However, the area is larger than that found in the single-station joint inversion in our previous paper. This means that the constraint on the parameters by the supposition of layer continuity is not as strong as in the case of single-station joint inversion. However, it can be concluded that multi-station joint inversion can avoid ambiguity in deep structure parameters, despite the lack of enough long-period phase velocity data.

Table 1. Subsurface structural model and search limits for a numerical experiment.
Site A and Site B have different layer thicknesses, so that we can confirm the applicability of the multi-station joint inversion method.

	True model					Search area	
Layer	V_p [km s^{-1}]	V_s [km s^{-1}]	Site A H [km]	Site B H [km]	ρ [t m^{-3}]	V_s [km s^{-1}]	H [km]
1	1.96	0.6	0.3	0.3	1.8	0.4–0.7	0.2–0.5
2	2.40	1.0	1.0	1.5	2.0	0.7–1.3	0.5–2.0
3	3.29	1.8	0.7	1.0	2.3	1.3–2.0	0.5–1.5
4	4.62	3.0	∞	∞	2.5	3.0	∞

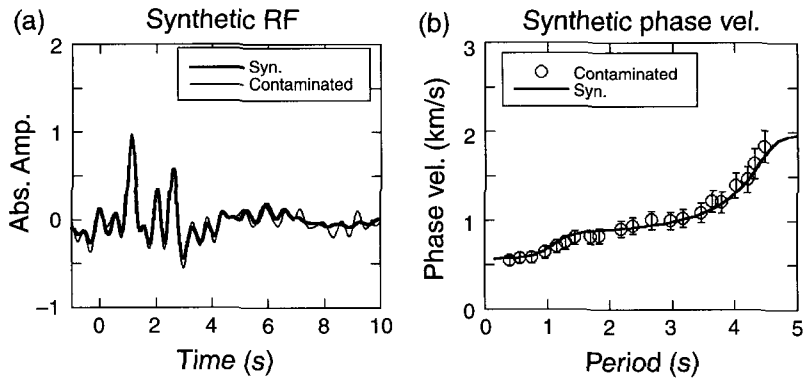

Fig. 2. Comparison of receiver function and fundamental-mode Rayleigh-wave phase velocity data for the model in Table 1 with those computed for a numerical test. (a) Receiver function for the true model for Site A (thin line) and noisy test data (thick line). (b) Phase velocity for the true model for Site B (thin line) and noisy test data (circles).

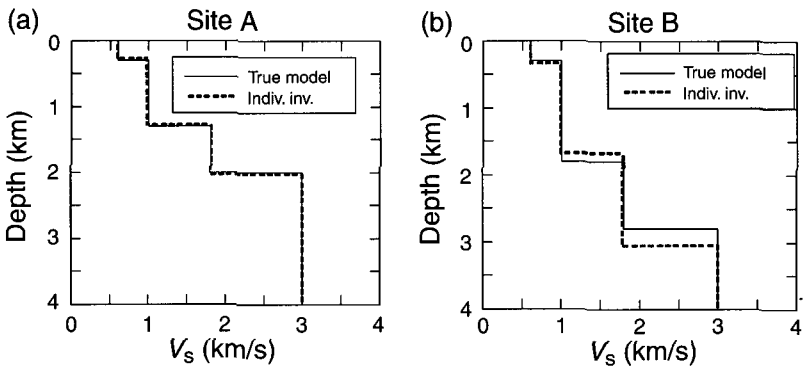

Fig. 3. Comparison of the true model and the models obtained by individual inversion of (a) receiver function data and (b) phase velocity data.

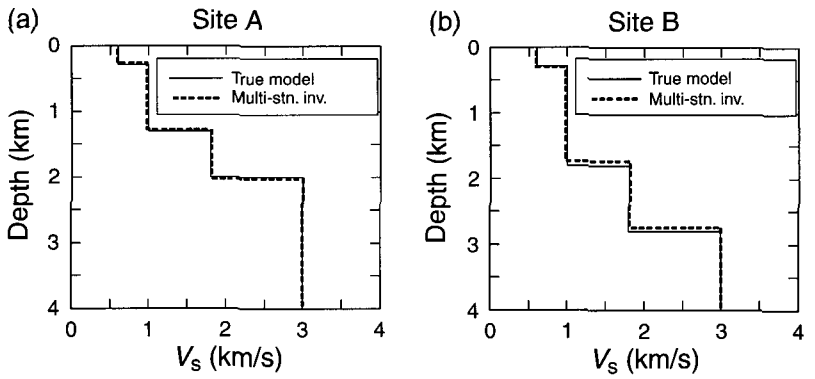

Fig. 4. Comparison of the true model and the model derived by multi-station joint inversion of receiver function and phase velocity data.

Application of multi-station joint inversion to observed data

We apply the multi-station joint inversion method to receiver function and phase velocity data observed in central Tokyo, Japan, where there are many seismological stations installed and many seismograms have been recorded through long-term observation. We derived receiver functions from earthquake records obtained at the Tokyo Observatory of the Japan Meteorological Agency (JMA TOKYO, shown in Figure 8), as in our previous paper. Rayleigh-wave phase velocity datasets were acquired from microtremor array surveys carried out at two sites, KOTO and SHIBUYA, in downtown Tokyo (Figure 8).

Receiver function observed at JMA TOKYO

The observed receiver function used here is almost the same as the one used in our previous paper. Earthquake data used in the derivation of the receiver function were acquired during the earthquakes that occurred in the east, off Izu Peninsula, as shown in Table 2 and Figure 8b. The water-level method (Langston, 1979) was applied to three-component records of the first 10 s from the P-wave onsets, and a band-pass filter with a period range from 0.5 to 5.0 s was applied during the calculation. These receiver functions were then stacked to form an average receiver function. The first 6 s of the averaged receiver function was used in the subsequent multi-station joint inversion, since usable

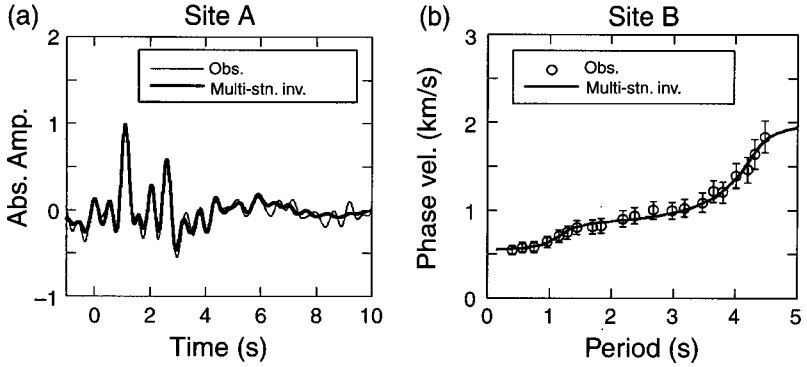

Fig. 5. Comparison between the data computed for a numerical test and the synthetic data obtained from a model resulting from multi-station joint inversion. (a) Receiver function at Site A. (b) Rayleigh-wave phase velocity at Site B.

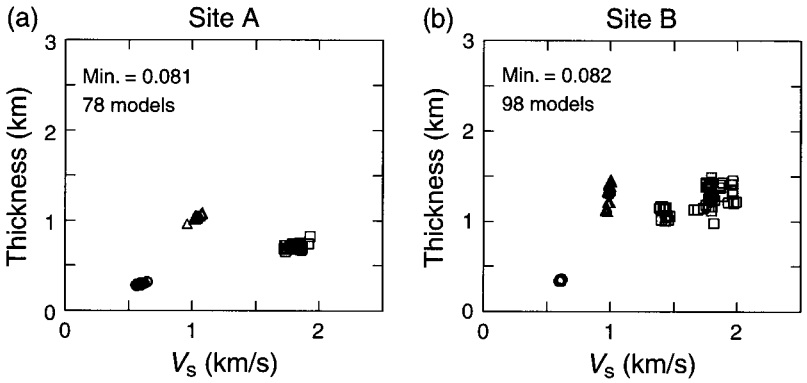

Fig. 6. Distribution of parameters in acceptable solutions for individual inversion of (a) receiver functions and (b) phase velocity, using numerical test data. Circles, triangles, and squares indicate the parameters of the first, second, and third layers, respectively. The acceptability threshold was set to be equal to the minimum misfit plus 0.01. The number of acceptable solutions and the minimum misfit value is also shown in each figure.

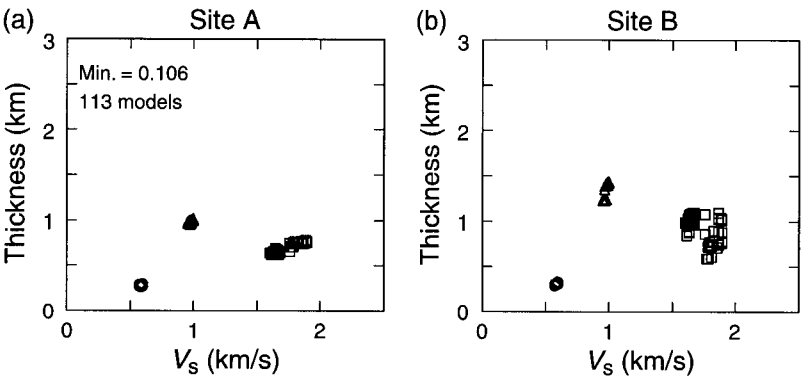

Fig. 7. Distribution of parameters in acceptable solutions for multi-station joint inversion, using numerical test data. Circles, triangles, and squares indicate the parameters of the first, seconds and third layers, respectively. The acceptability threshold was set to be equal to the minimum misfit plus 0.01. Because the multi-station joint inversion fits data from both sites with one single model, only one group of acceptable solutions and one minimum misfit value are obtained, as shown in Figure 7a.

phases of the receiver function are limited to this time range. The resultant receiver function is presented in Figure 9a. Refer to our previous paper for details of the observed receiver function used here.

Phase velocity dispersion observed at KOTO

Yamanaka et al. (1995) performed a microtremor array survey in central Tokyo, at the KOTO site shown in Figure 8a. They obtained Rayleigh-wave phase velocity at periods from 0.8 to 4.3 s. They inferred an S-wave velocity profile by inversion of the phase velocity dispersion data, which indicated that the basement depth is ~2.1 km, shallower than found in a seismic refraction survey (Koketsu, 1995) or deep borehole data (Suzuki, 1999). Because the long-period phase velocity observed at this site was not well resolved, with large values of standard deviation, an invalid structural model with shallower basement depth was found. Therefore in the multi-station joint inversion here we use only Rayleigh-wave phase velocity data at periods

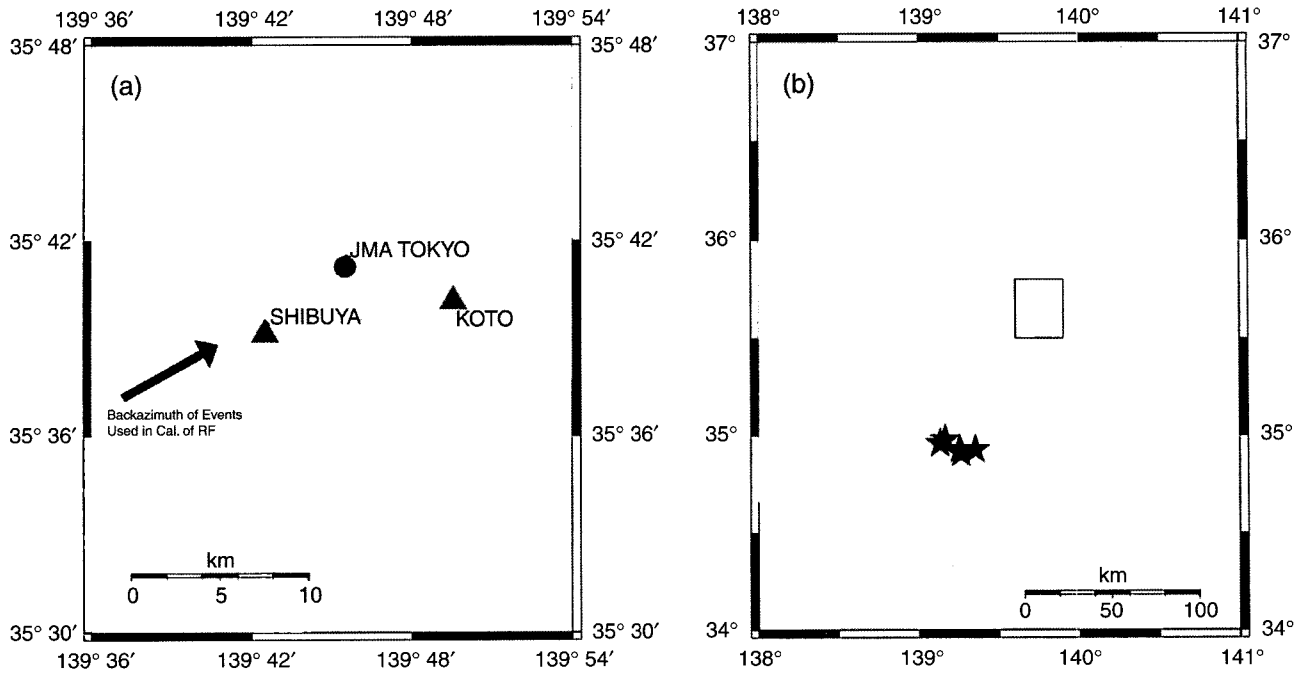

Fig. 8. Map of stations and epicentres. (a) Location of Tokyo Observatory of the Japan Meteorological Agency (JMA TOKYO), and the microtremor array sites, KOTO (Yamanaka et al., 1995) and SHIBUYA (Yamanaka and Yamada, 2002). The map also shows back-azimuth directions of earthquakes used in calculation of receiver function. (b) Location of epicentres of earthquakes used in the calculation of receiver functions. The rectangle corresponds to the area shown in Figure 8a.

Table 2. List of earthquakes used in calculation of receiver functions. Δ is the epicentral distance and θ is the back-azimuth.

From Kurose and Yamanaka (2006).

No.	Date [dd mon yyyy]	Time	Lat. [°]	Lon. [°]	D [km]	M	Δ [km]	θ [deg]
1	01 Aug 1988	1:10	34.93	139.25	23	4.2	96	209
2	05 Jul 1989	2:28	34.91	139.26	48	4.3	98	207
3	07 Jul 1989	0:01	34.98	139.16	21	5.3	95	215
4	09 Jul 1989	11:09	34.96	139.13	24	5.5	99	215
5	22 Jan 1995	17:01	34.93	139.35	28	4.0	92	203

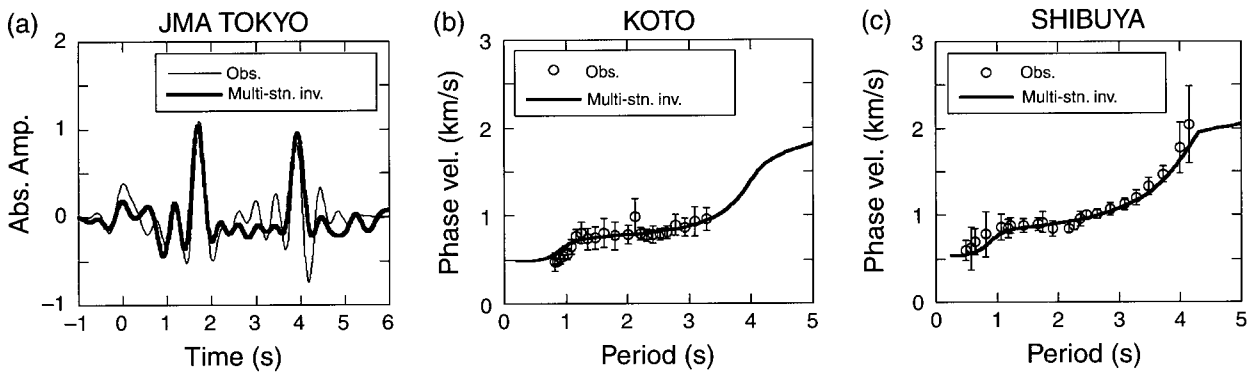

Fig. 9. Comparison of observations and synthetic data obtained from the result of multi-station joint inversion. (a) Receiver function at JMA TOKYO. (b) Rayleigh-wave phase velocity dispersion at KOTO. (c) Rayleigh-wave phase velocity at SHIBUYA.

shorter than 3.5 s, with small values of the standard deviation as shown in Figure 9b.

Phase velocity observed at SHIBUYA

Yamanaka and Yamada (2002) conducted a microtremor array survey in central Tokyo, at the SHIBUYA site shown in Figure 8a. They derived Rayleigh-wave phase velocities at periods from 0.5 to 4.2 s, as shown in Figure 9c. They also deduced an S-wave velocity profile by inversion of the dispersion curve, and estimated that the basement depth is ~2.5 km, which was consistent with the results of previous studies mentioned earlier.

Multi-station joint inversion

In the inversion, we assumed 3 layers over the basement, as in our previous paper, since there are 3 major geological units in this area; one is a Quaternary layer and the other two units are of Tertiary age. Table 3 presents the search limits for S-wave velocities and thicknesses in the genetic algorithm inversion.

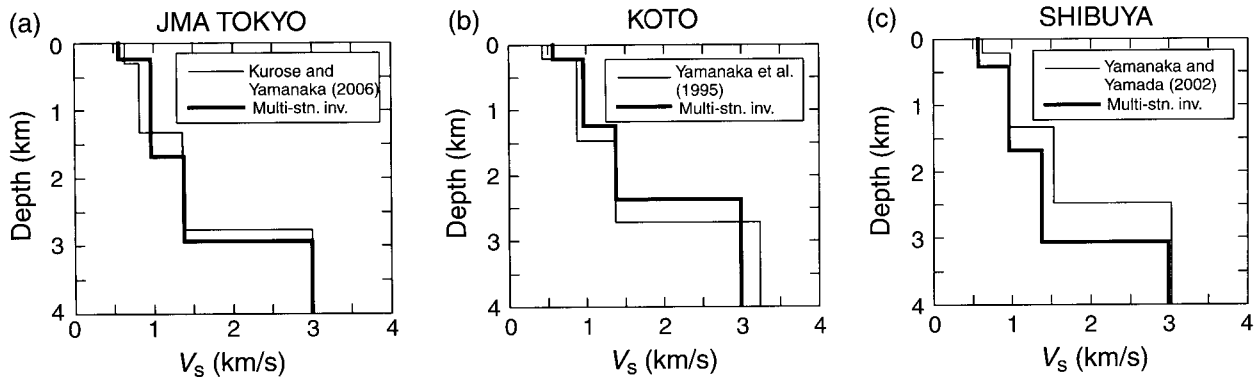

Fig. 10. Comparison between the profiles obtained by the multi-station joint inversion and those found by previous studies. The previous studies are by (a) Kurose and Yamanaka (2006), (b) Yamanaka et al. (1995), and (c) Yamanaka and Yamada (2002), respectively.

These limits were determined by reference to some previous studies about subsurface structure in and around Tokyo, Japan (Yamanaka et al., 1995; Yamanaka and Yamada, 2002). The angle of incidence of P-waves at the sediment/basement interface was set to be 34.6° in the calculation of the receiver function, as in our previous paper.

Figures 10 and 11 illustrate the subsurface structural models obtained by the multi-station joint inversion. The estimated basement depth is between 2.5 and 3.0 km at the three sites, in agreement with the results of the deep borehole investigation (Suzuki, 1999). The inversion models are compared with those from previous studies in Figure 10. At JMA TOKYO and KOTO, the new models are fairly consistent with those from previous studies, while the inversion model at SHIBUYA has deeper layer boundaries than found by the previous study.

In Figure 9 the observations and the synthetic data obtained from the result of multi-station joint inversion at each site are compared. The inversion result does approximately explain the observed data at all the sites, even at SHIBUYA, where the estimated layer boundaries are deeper than found previously. At KOTO, the synthetic phase velocities are slightly larger than the observed data at shorter periods. On the other hand, the observed phase velocity at SHIBUYA is larger than the synthetic data at periods less than 1 s. In the receiver function at JMA TOKYO, the amplitude of the phase corresponding to the direct P-wave ($t = 0$) is underestimated by the inversion result. The individual inversion of the receiver function at JMA TOKYO, not shown here, gave a model with S-wave velocity in the first layer $\sim 0.7\,\mathrm{km\,s^{-1}}$, which is larger than that of the multi-station inversion result shown here. However, inversion of the receiver function alone reproduced well the amplitude of the direct P-wave phase. Therefore, it is considered that these differences between the observed and synthetic data are chiefly attributable to near-surface structure, which seems to show that the near-surface structure here differs from site to site. In the previous study, the S-wave velocity of the first layer at KOTO was estimated to be $\sim 0.4\,\mathrm{km\,s^{-1}}$ (Figure 10b), and at JMA TOKYO, the S-wave velocity was $0.7\,\mathrm{km\,s^{-1}}$ in the first layer, as shown in Figure 10a. In fact, the KOTO site is located in a coastal area covered with soft soils, while the JMA TOKYO and the SHIBUYA sites are situated on comparatively stiff deposits, suggesting a substantial difference of the near-surface structure among these sites. However, multi-station joint inversion assumes S-wave velocity in each layer is uniform, and so does not take local differences in near-surface structure into consideration, which results in an averaged S-wave velocity profile.

Figure 12 illustrates the parameter distributions for the acceptable solutions obtained from multi-station joint inversion. The misfit criterion for determining acceptable models was set to be equal to the value of the minimum misfit plus 0.06. The parameters for all the layers at the sites of JMA TOKYO and SHIBUYA are distributed in very small areas, with only slight deviations in the deep part of the structure. This indicates that there is a very narrow and deep depression in the misfit surface, corresponding with the global minimum, without any other local misfit minima comparable to the global minimum, and this guarantees the uniqueness of the final model. At the KOTO site, the parameters, especially for the deeper layers, are distributed over a large area, which shows the deterioration of resolution of thickness in deeper layers, similar to the results for individual inversion at a single site. This is considered to be because we used phase velocities for short periods only at this site, which

Table 3. Search limits for S-wave velocity and thickness parameters in multi-station joint inversion of receiver function and Rayleigh-wave phase velocity data, to estimate the S-wave velocity profile in central Tokyo, Japan.

Layer	V_S [km s^{-1}]	H [km]	ρ [t m^{-3}]
1	0.4–0.6	0.2–0.6	1.8
2	0.8–1.0	0.8–2.0	1.9
3	1.3–1.6	0.8–2.0	2.0
4	3.0	∞	2.5

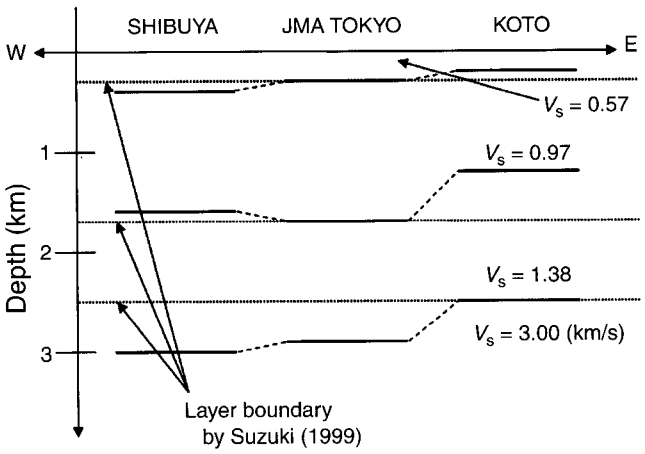

Fig. 11. Schematic diagram of subsurface structure in central Tokyo, Japan, estimated from multi-station joint inversion of receiver function and surface-wave phase velocity data.

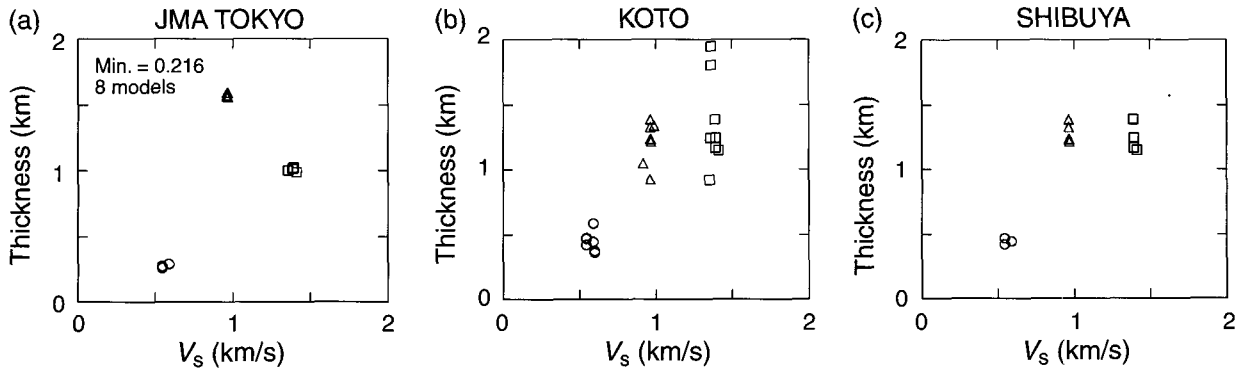

Fig. 12. Distribution of parameters of acceptable solutions for multi-station joint inversion. Circles, triangles, and squares indicate the parameters of the first, second, and third layers, respectively. The acceptability threshold was set to be equal to the minimum misfit plus 0.06. Because multi-station joint inversion fits the data at all three sites with one single model in this case, only one group of acceptable solutions and one minimum misfit value are obtained, as displayed in Figure 12a.

hardly constrains the deep structure. This suggests that there is a limitation to the ability of our multi-station joint inversion method to overcome the ambiguity of deep structure. However, the resolution of thickness differs from site to site, and this should be evaluated by an appropriate method, such as our multi-station joint inversion, especially where there is insufficient long-period surface-wave dispersion data.

Discussion

In this study, we have proposed multi-station joint inversion of receiver function and surface-wave phase velocity data observed at several different sites, using genetic algorithms, in order to accurately estimate the S-wave velocity structure of deep sedimentary layers, down to the basement which has an S-wave velocity of ~3.0 km s^{-1}. Numerical experiments demonstrated that the proposed method could overcome the non-uniqueness of the inversion result that arises when modelling only one kind of observed data. The method was also effective in reducing the lack of resolution of deep structure when inverting phase velocity dispersion over a limited period range only. Application of the method to actual data obtained in central Tokyo, Japan, led to good agreement with the results of previous studies. These are the same advantages as shown by joint inversion of receiver function and phase velocity data at a single station (Kurose and Yamanaka, 2006). Multi-station joint inversion allows data obtained at different sites to be used and so is more applicable than joint inversion at a single station.

However, the assumption of uniformity of S-wave velocity in each layer gave rise to the problem that the method cannot describe the detailed variation in local near-surface structure. In order to cope with this problem, the assumption by Feng et al. (2003) that S-wave velocity be allowed to change within a prescribed range, even in the same layer, may be helpful. It may also be worth investigating a method in which the S-wave velocity in the first layer is determined absolutely independently at each site, for example using individual inversion of receiver function or phase velocity data at each site, and that S-wave velocity for the second and the third layers be constrained to be common to all the sites.

There are other problems related to the assumption of layer continuity in the method. One of them is how to validate layer continuity before the method is applied to an area in which little *a priori* information on subsurface structure available. Another problem is how the method might be applied to an area with horizontally-discontinuous layers. These problems may be settled to some extent by first performing individual inversions at each site to outline the subsurface structure of the target area, and then conducting a multi-station joint inversion with a starting model based on the results of the prescribed individual inversions. In spite of these difficulties, the method is still useful in establishing a 3D basin model for use in prediction of strong ground motion. Since homogeneous layers are often assumed in such models, our method can provide an averaged velocity model of a basin that does explain observed phase velocities and receiver functions.

Acknowledgments

The authors thank Yoshihiro Kinugasa and Kenichiro Kusunoki for helpful advice and guidance in improving this paper. The thought-provoking comments from reviewers are also appreciated. Earthquake records used in this study were obtained by Japan Meteorological Agency. This study is supported in part by a Grant-in-Aid for General Scientific Research (nos. 14206081, 15510147) and Special Project for Earthquake Disaster Mitigation in Urban Areas from Japanese Ministry of Education, Culture, Sports, Science and Technology.

References

Ammon, C. J., Randall, G. R., Zandt, G., 1990, On the nonuniqueness of receiver function inversion: *Journal of Geophysical Research* **95**, 15303–15318.

Chang, S.-J., Baag, C.-E., Langston, C. A., 2004, Joint analysis of teleseismic receiver function and surface wave dispersion using genetic algorithm: *Bulletin of the Seismological Society of America* **94**, 691–704. doi: 10.1785/0120030110

Cho, I., Nakanishi, I., Ling, S., Okada, H., 1999, Application of Forking Genetic Algorithm fGA to an exploration method using microtremors: *Geophysical Exploration (Butsuri-Tansa)* **52**, 227–246.

Darbyshire, F. A., Priestley, K. F., White, R. S., Stefansson, R., Gudmundsson, G. B., Jakobsdottir, S. S., 2000, Crustal structure of central and northern Iceland from analysis of teleseismic receiver functions: *Geophysical Journal International* **143**, 163–184. doi: 10.1046/j.1365-246x.2000.00224.x

Feng, S., Sugiyama, T., Yamanaka, H., 2003, Multi-station inversion in array microtremor survey: *Geophysical Exploration (Butsuri-Tansa)* **56**, 1–11.

Haskell, N. A., 1953, The dispersion of surface waves in multilayered media: *Bulletin of the Seismological Society of America* **43**, 17–34.

Haskell, N. A., 1962, Crustal reflection of plane P and SV waves: *Journal of Geophysical Research* **67**, 4751–4767.

Horike, M., 1985, Inversion of phase velocity of long-period microtremors to the S wave velocity structure down to the basement in urbanized areas: *Journal of Physics of the Earth* **33**, 59–96.

Julia, J., Ammon, C. J., Herrmann, R. B., Correig, A. M., 2000, Joint inversion of receiver function and surface wave dispersion observations: *Geophysical Journal International* **143**, 99–112. doi:10.1046/j.1365-246x.2000.00217.x

Kagawa, T., Sawada, S., Iwasaki, Y., Nanjo, A., 1998, S-wave velocity structure model of the Osaka sedimentary basin from microtremor array observations: *Journal of the Seismological Society of Japan (Zisin)* **51**, 31–40.

Kitsunezaki, C., Goto, N., Kobayashi, Y., Ikawa, T., Horike, M., Saito, T., Kurota, T., Yamane, K., Okuzumi, K., 1990, Estimation of P- and S-wave velocities in deep soil deposits for evaluating ground vibrations in earthquake: *Journal of Natural Disaster Science* **9**(3), 1–17.

Kobayashi, K., Uetake, T., Mashimo, M., Kobayashi, H., 1998, An investigation on detection method of P to S converted waves for estimating deep underground structures: *Journal of Structural and Construction Engineering* **505**, 45–52.

Koketsu, K., 1995, Underground structure in the Tokyo metropolitan area: *Geophysical Exploration (Butsuri-Tansa)* **48**, 504–518.

Kurose, T., Yamanaka, H., 2006, Joint inversion of receiver function and surface-wave phase velocity for estimation of shear-wave velocity of sedimentary layers: *Geophysical Exploration (Butsuri-Tansa)* **59**, 93–101.

Langston, C. A., 1979, Structure under Mount Rainier, Washington, inferred from teleseismic bodywaves: *Journal of Geophysical Research* **84**, 4749–4762.

Last, R. J., Nyblade, A. A., Langston, C. A., Owens, T. J., 1997, Crustal structure of the East African Plateau from receiver functions and Rayleigh wave phase velocities: *Journal of Geophysical Research* **102**, 24469–24483. doi:10.1029/97JB02156

Lomax, A., Snieder, R., 1994, Finding of acceptable solutions with a genetic algorithm with application of surface wave group velocity dispersion in Europe: *Geophysical Research Letters* **21**, 2617–2620. doi:10.1029/94GL02635

Okada, H., 2003, *The microtremor survey method*, Society of Exploration Geophysicists.

Owens, T. J., Zandt, G., Taylor, S. R., 1984, Seismic evidence for an ancient rift beneath the Cumberland Plateau, Tennessee: A detailed analysis of broadband teleseismic P waveforms: *Journal of Geophysical Research* **89**, 7783–7795.

Priestley, K. F., Zandt, G., Randall, G. E., 1988, Crustal structure in Eastern Kazakh, U.S.S.R. from teleseismic receiver function: *Geophysical Research Letters* **15**, 613–616.

Suzuki, H., 1999, Deep geological structure and seismic activity in the Tokyo metropolitan area: *Journal of Geography* **108**, 336–339.

Yamanaka, H., Furuya, S., Nozawa, T., Sasaki, T., Takai, T., 1995, Array measurements of long-period microtremors in the Kanto Plain – Estimation of S-wave velocity structure at Koto: *Journal of Structural and Construction Engineering* **478**, 99–105.

Yamanaka, H., Ishida, H., 1996, Application of genetic algorithms to an inversion of surface-wave dispersion data: *Bulletin of the Seismological Society of America* **86**, 436–444.

Yamanaka, H., Yamada, N., 2002, Estimation of 3D S-wave velocity model of deep sedimentary layers in Kanto plain, Japan, using microtremor array measurements: *Geophysical Exploration (Butsuri-Tansa)* **55**, 53–65.

Manuscript received 1 August 2006; accepted 20 October 2006.

レシーバー関数と表面波位相速度の多地点同時逆解析による深部地盤構造の推定

黒瀬 健[1]・山中 浩明[2]

要 旨： 本研究では，地震基盤に至る深部地盤構造の推定を目的として，レシーバー関数と表面波位相速度の多地点同時逆解析手法を提案し，その適用性を検討している。提案手法は，堆積平野の地下における各層の物性値（特にＳ波速度）を一様であると仮定することで，層の連続性を考慮し，複数地点で得られたレシーバー関数及び位相速度の観測データを同時に逆解析するものである。地震基盤までの深部地下構造を模擬したモデルから，レシーバー関数及び基本モードのレイリー波の位相速度を計算し，ランダムノイズを加えたものを擬似観測値として提案手法の数値実験を行った。その結果，提案手法によってＳ波速度と層厚の間のトレードオフの影響が軽減されることがわかった。次に，東京都都心部で観測された地震記録から得られたレシーバー関数と，微動アレイ探査によって得られた位相速度との多地点同時逆解析を行い，深部地盤構造を推定した。推定された地下構造は，既存の探査結果と概ね一致しており，提案手法の妥当性が確認された。また，レシーバー関数及び位相速度の単点での単独逆解析における解の非一意性の問題が解決されることが確認された。

キーワード：多地点同時逆解析，レシーバー関数，表面波，位相速度，アレイ微動探査，Ｓ波速度，遺伝的アルゴリズム

심부 퇴적층 탐사를 위한 수신함수와 표면파 위상속도를 이용한 다측점 자료의 복합 역산

Takeshi Kurose[1] and Hiroaki Yamanaka[2]

요 약： 이 연구에서는 심부 퇴적층의 S-파 속도구조 추정을 위하여 여러 지점에서 획득된 수신함수와 표면파 위상속도 자료를 이용하는 유전자 알고리즘 기반 복합 역산기법을 제안하였다. 이 방법은 서로 다른 지점에서 획득된 자료를 동시에 역산하기 위해, 역산대상 지역 내 모든 측점 상부의 지층 물성 - 특히 S-파 속도 –이 균일하다고 가정하는 방식으로 역산대상 지역 상부층의 층서적 연속성을 고려한다. 인공합성 자료를 이용한 수치실험 결과, 본 방법은 제한된 주기대역을 가지는 표면파 위상속도 자료만을 모델링 할 때 발생하는 심부 지층 물성정보에 대한 불확실성을 효과적으로 줄일 수 있음을 보여주었다. 또한 본 연구에서는 한 지점에서 획득된 지진파 기록으로부터 구해진 수신함수와, 일본 동경 중부지역에서 수행된 미소진동탐사로부터 획득된 두 개의 레일리파 위상속도 자료에 대해 제안된 기법을 적용하였다. 그 결과, 추정된 지하 구조는 선행된 탄성파 굴절법 탐사와 심부 시추공 자료와 잘 일치하는 양상을 보여주었다. 이러한 측면에서, 제안된 방법은 수신함수만을, 혹은 표면파 위상속도 자료만을 이용하는 개별역산에 비해 보다 정확하고 신뢰할 수 있는 모델을 제공하는 방법이 될 수 있을 것으로 판단된다.

주요어： 다측점 복합역산, 수신함수, 표면파, 위상속도, 미소진동탐사, S-파 속도, 유전자 알고리즘

1 東京工業大学 総合理工学研究科
（現、伊藤忠テクノソリューションズ（株））
2 東京工業大学 総合理工学研究科

1 토쿄공업대학 종합이공학연구과
(Presently, ITOCHU Techno-Solutions Corp. Ltd.)
2 토쿄공업대학 종합이공학연구과